Manuscript submitted to Chemical Engineering Science

General pure convection residence time distribution theory of fully developed laminar flows in straight planar and axisymmetric channels

Martin Wörner

Karlsruhe Institute of Technology (KIT), Institute of Catalysis Research and Technology,

Hermann-von-Helmholtz-Platz 1, 76344 Eggenstein-Leopoldshafen, Germany

E-mail: martin.woerner@kit.edu, Phone +49 721 608 47426, Fax: +49 721 608 44805

Highlights

- The diffusion-free RTD of fully developed laminar flow is studied analytically
- A general relation for computing the RTD of a given 1D velocity profile is derived
- The relation applies to straight planar and axisymmetric channels
- The theory is unifying and comprises all pure convection RTDs derived so far
- The theory is used to derive the RTD of general plane Couette-Poiseuille flow

Graphical Abstract

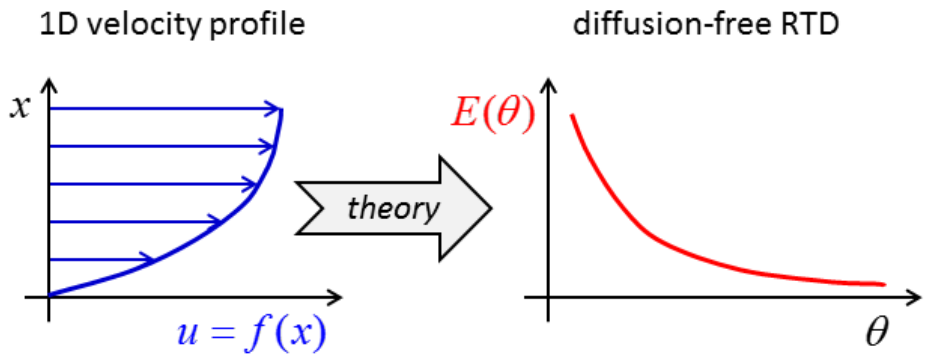

Abstract

In literature, the diffusion-free residence time distribution (RTD) of laminar flows - the so-called convection model - has been determined for various velocity profiles mostly on a case-by-case basis. In this analytical paper, we derive general mathematical relations which allow computing the diffusion-free differential and cumulative RTD in straight planar, circular and concentric annular channels for arbitrary monotonic and piece-wise monotonic one-dimensional velocity profiles. The theory is used to determine the RTD of plane Couette-Poiseuille flow with non-monotonic velocity profile, and the optimal value of the volumetric flow rate where the RTD becomes most narrow. It is shown that any velocity profile that depends in a sub-layer linearly on the distance from a stationary or moving no-slip wall has a differential RTD which follows a -3 power law as the residence time approaches its maximum. The variance of the RTD is directly associated with the asymptotic behavior of the RTD and can be finite or infinite.

Keywords: Residence time distribution; Laminar flow; Pure convection model; Macromixing

1. Introduction

Reactors with laminar flow are frequently used for processing viscous fluids such as liquid food products (Torres and Oliveira, 1998) or polymers (Gogos et al., 1987), and in micro process engineering (Kockmann, 2006). Recent progress in microfluidic technology has turned attention to the residence time distribution (RTD) in micro-devices (Cantu-Perez et al., 2010; Lohse et al., 2008; Vikhansky, 2011; Wibel et al., 2013). The velocity profile of laminar flow causes fluid elements to spent different times within the reactor and gives rise to a wide RTD. In the pure convection regime, molecular diffusion is negligible and each fluid element follows its streamline with no intermixing with neighboring elements. This corresponds to 'macrofluid behaviour' so that the average conversion can be predicted by the total segregation model (Danckwerts, 1958; Fogler, 1986; Zwietering, 1959). This model assumes that fluid elements having the same age (residence time) 'travel together' in the reactor and do not mix with elements of different ages until they exit the reactor (Madeira et al., 2006). Levenspiel (1999) provides a map which recommends using the pure convection model for situations, where the Bodenstein number is sufficiently large while the ratio between channel length and diameter is sufficiently low.

In this paper we are interested in the RTD of this pure convective regime for general laminar flows. Throughout the paper we assume that the ratio of the length to the hydraulic diameter of the channel is sufficiently long so that entrance effects can be ignored; for a discussion of entrance effects on the RTD we refer to Ham et al. (2011). Under these conditions, the cumulative RTD, $F(\theta)$, and the non-dimensional differential RTD, $E_\theta(\theta) = \mathrm{d}F(\theta)/\mathrm{d}\theta$, depend on the fully developed velocity profile only and are fully deterministic. Closed analytical forms of the diffusion-free RTD in laminar flows are known only for very few channel shapes and certain Newtonian, non-Newtonian or generalized velocity profiles, see Table 1. Examples are axisymmetric flows in a circular pipe (Bosworth, 1948; Danckwerts, 1953; Delaplace et al., 2008; Hsu and Wei, 2005; Osborne, 1975; Pegoraro et al., 2012; Sawinsky and Balint, 1984; Sawinsky and Deak, 1995; Wein and Ulbrecht, 1972; Zakharov, 2006), in

a planar channel (Asbjornsen, 1961; Levenspiel et al., 1970; Sawinsky and Simandi, 1983; Zakharov, 2006) and in a concentric annulus (Nigam and Vasudeva, 1976). In all these cases the velocity profile is one-dimensional as it depends on one co-ordinate only. For fully developed two-dimensional laminar flows, the diffusion-free RTD has been obtained approximately for helically coiled tubes (Nauman, 1977) and rectangular channels (Wörner, 2010), and analytically exact for channels with moon-shaped cross-section (Erdogan and Wörner, 2013).

The mathematical procedure to compute the RTD from the given laminar velocity profile is always similar. However, it has been applied mostly in a case-by-case manner. While Wein and Ulbrecht (1972) and Nauman (1974) derived a general expression for computing the RTD from a given monotonic velocity profile in a circular pipe flow, their relations are almost unknown to the community and have obviously not been used by other authors so far. In this paper we extend these studies and derive, for the first time, an explicit relation which allows computing the RTD from arbitrary one-dimensional monotonic or non-monotonic (but piecewise monotonic) laminar velocity profiles in planar, circular and annular channels. This relation includes all previous results from literature as special cases.

In Section 2 of this paper we give some basic definitions and provide a general mathematical expression for computing the convection model RTD from a given laminar velocity profile. In Section 3 we apply the new theory and determine for various velocity profiles the corresponding RTD. We recover some known results from literature but also present new results not obtained so far. In Section 4 we discuss the implications of the theory on the asymptotic behaviour and the variance of the RTD. The paper closes by a short summary and conclusions in Section 5.

2. General pure convection RTD theory

2.1. Basic definitions

We consider a straight flow domain with length L, constant cross sectional area A, volume $V = LA$, constant total volumetric flow rate Q_{total}, mean velocity $U_{\text{m}} = Q_{\text{total}} / A$, and mean (hydrodynamic) residence time $t_{\text{m}} = V / Q_{\text{total}} = L / U_{\text{m}}$. We assume that the flow in this domain is steady, unidirectional (axial) and obeys a given fully developed laminar one-dimensional velocity profile.

In the sequel, we express all results in terms of the non-dimensional time $\theta = t / t_{\text{m}}$. The non-dimensional residence time of the fastest fluid elements is commonly denoted as first-appearance time or break-through time; it is given by $\theta_{\text{F}} = U_{\text{m}} / U_{\max}$, where $U_{\max}$ is the maximum velocity of the profile. For $\theta < \theta_{\text{F}}$ it is $E_\theta = F = 0$; the equations given for E_θ and F in the remainder of the paper refer to $\theta \geq \theta_{\text{F}}$ only.

For any RTD, the zero and first moment are unity, i.e.

$$\mu_0 = \int_0^\infty E_\theta \mathrm{d}\theta = 1, \quad \mu_1 = \int_0^\infty \theta E_\theta \mathrm{d}\theta = 1 \tag{1}$$

The definition of the variance is

$$\sigma_\theta^2 = \int_0^\infty \left(\theta - 1\right)^2 E_\theta \mathrm{d}\theta = -1 + 2\int_0^\infty \theta(1-F)\mathrm{d}\theta = -1 + \theta_{\text{F}}^2 + 2\int_{\theta_{\text{F}}}^\infty \theta(1-F)\mathrm{d}\theta \tag{2}$$

In the absence of diffusion, species transport is by convection only and the differential and cumulative RTD are given by

$$E_\theta \mathrm{d}\theta = \frac{\mathrm{d}Q(\theta)}{Q_{\text{total}}}, \qquad F(\theta) = \frac{Q(\theta)}{Q_{\text{total}}} \tag{3}$$

Here, $Q(\theta)$ is the volumetric flow rate associated with a residence time θ or lower (Wein and Ulbrecht, 1972).

2.2. Analytical RTDs for one-dimensional velocity profiles

In this paper, we consider three types of channels, namely parallel plates with distance $H_{\parallel}$, a circular pipe with radius R, and a concentric annulus with outer radius R and inner radius αR, where $0 < \alpha < 1$. For normalization, we use either $H_{\parallel}$ or R as length scale and U_{m} as velocity scale. The non-dimensional velocity $\hat{u} = u / U_{\mathrm{m}} = f(\hat{y})$ is a function of the non-dimensional lateral coordinate $\hat{y}$, which is in the range $\hat{y}_{\min} \le \hat{y} \le 1$. For the planar channel and the pipe it is $\hat{y}_{\min} = 0$ and for the annulus $\hat{y}_{\min} = \alpha$. The velocity values at the lower and upper boundaries of the flow domains are $\hat{u}_0 = \hat{u}(\hat{y}_{\min}) = U_0 / U_{\mathrm{m}}$ and $\hat{u}_1 = \hat{u}(\hat{y} = 1) = U_1 / U_{\mathrm{m}}$, respectively.

With these definitions, the non-dimensional residence time of fluid elements at position $\hat{y}$ is

$$\theta = \frac{L/u}{t_{\mathrm{m}}} = \frac{1}{\hat{u}} = \frac{1}{f(\hat{y})} \tag{4}$$

In the sequel, we need the inverse relation of Eq. (4). We denote the inverse function of f as f^{-1} so that $\hat{y} = f^{-1}(\theta^{-1})$ and distinguish two types of velocity profiles.

2.2.1. Monotonic velocity profile with maximum at one boundary

In the first case, the maximum velocity $U_{\max}$ is located at one boundary (here we choose the lower one $\hat{y}_{\min}$) while the minimum velocity $U_{\min}$ is located at the other boundary (here the upper one $\hat{y} = 1$). In this case f is strictly monotonic decreasing from $f(\hat{y}_{\min}) = \theta_{\mathrm{F}}^{-1}$ to $f(1) = U_{\min} / U_{\mathrm{m}}$ so that f^{-1} is unique. The region that is associated with a residence time θ or lower is $\hat{y}_{\min} \le \hat{y} \le \hat{y}_{+}$ so that

$$F(\theta) = \frac{1}{A} \int_{\hat{y}_{\min}}^{f^{-1}(\theta^{-1})} f(\hat{y}) \mathrm{d}A = \int_{\hat{y}_{\min}}^{f^{-1}(\theta^{-1})} (2\hat{y})^{\kappa} f(\hat{y}) \mathrm{d}\hat{y} \tag{5}$$

Here, we used the relation $\mathrm{d}A / A = (2\hat{y})^{\kappa} \mathrm{d}\hat{y}$ with $\kappa = 0$ for the planar channel and $\kappa = 1$ for the pipe and annulus. Partial integration of the right-hand-side of Eq. (5) gives

$$F(\theta) = (2 f^{-1}(\theta^{-1}))^{\kappa} G(f^{-1}(\theta^{-1})) - (2\hat{y}_{\min})^{\kappa} G(\hat{y}_{\min}) - 2\kappa \left[H(f^{-1}(\theta^{-1})) - H(\hat{y}_{\min}) \right] \tag{6}$$

where G is the antiderivative of f and H is the antiderivative of G.

The differential RTD is given by

$$E_{\theta} = \frac{\mathrm{d}F(\theta)}{\mathrm{d}\theta} = \frac{\mathrm{d}}{\mathrm{d}\theta} \int_{\hat{y}_{\min}}^{f^{-1}(\theta^{-1})} (2\hat{y})^{\kappa} f(\hat{y}) \mathrm{d}\hat{y} = (2 f^{-1}(\theta^{-1}))^{\kappa} f(f^{-1}(\theta^{-1})) \cdot \left. \frac{\mathrm{d}\hat{y}}{\mathrm{d}\theta} \right|_{f^{-1}(\theta^{-1})} \tag{7}$$

With $f(f^{-1}(\theta^{-1})) = \theta^{-1}$ and

$$\frac{\mathrm{d}\hat{y}}{\mathrm{d}\theta} = \frac{\mathrm{d}\hat{y}}{\mathrm{d}\hat{u}} \frac{\mathrm{d}\hat{u}}{\mathrm{d}\theta} = -\frac{1}{\theta^2} \frac{\mathrm{d}\hat{y}}{\mathrm{d}\hat{u}} = -\frac{1}{\theta^2 f'(\hat{y})} \tag{8}$$

Eq. (7) becomes

$$E_{\theta} = -\frac{1}{\theta^3} \frac{(2 f^{-1}(\theta^{-1}))^{\kappa}}{f'(f^{-1}(\theta^{-1}))} \tag{9}$$

2.2.2. Piecewise monotonic velocity profile with maximum within the channel

We now consider velocity profiles which have a maximum at a certain position within the channel and distinguish two cases. In the first case, the velocity profile is double-valued in the entire domain $\hat{y}_{\min} \le \hat{y} \le 1$. Then, f^{-1} has the two branches $\hat{y}_{-} = f_{-}^{-1}(\theta^{-1})$ and $\hat{y}_{+} = f_{+}^{-1}(\theta^{-1})$. The region that is associated with a residence time θ or lower is then given by $\hat{y}_{-} \le \hat{y} \le \hat{y}_{+}$ so that the cumulative RTD becomes

$$F(\theta) = \int_{f_{-}^{-1}(\theta^{-1})}^{f_{+}^{-1}(\theta^{-1})} (2\hat{y})^{\kappa} f(\hat{y}) \mathrm{d}\hat{y} \tag{10}$$

Partial integration of the right-hand-side of Eq. (10) gives

$$F(\theta) = (2 f_+^{-1}(\theta^{-1}))^\kappa G(f_+^{-1}(\theta^{-1})) - (2 f_-^{-1}(\theta^{-1}))^\kappa G(f_-^{-1}(\theta^{-1})) - 2\kappa\left[H(f_+^{-1}(\theta^{-1})) - H(f_-^{-1}(\theta^{-1})) \right] \quad (11)$$

The differential RTD is then given by

$$E_\theta = \frac{\mathrm{d}F(\theta)}{\mathrm{d}\theta} = \frac{\mathrm{d}}{\mathrm{d}\theta} \int_{f_-^{-1}(\theta^{-1})}^{f_+^{-1}(\theta^{-1})} (2\hat{y})^\kappa f(\hat{y}) \mathrm{d}\hat{y} = -\frac{1}{\theta^3} \left(\frac{(2 f_+^{-1}(\theta^{-1}))^\kappa}{f'(f_+^{-1}(\theta^{-1}))} - \frac{(2 f_-^{-1}(\theta^{-1}))^\kappa}{f'(f_-^{-1}(\theta^{-1}))} \right) \quad (12)$$

In the second case, the velocity profile is double valued in one part of the domain and is single-valued in the rest of the domain. Here, we assume that the double-valued part with the velocity maximum is in the region $\hat{y}_{\min} \le \hat{y} \le \hat{y}_{\mathrm{dv}}$ while the single-valued part is in region $\hat{y}_{\mathrm{dv}} < \hat{y} \le 1$. The cumulative and differential RTD are then given by Eq. (11) and (12) for $\theta \le \theta_{\mathrm{dv}} = 1/\hat{u}(\hat{y}_{\mathrm{dv}})$, whereas for $\theta > \theta_{\mathrm{dv}}$ we have

$$F(\theta) = \underbrace{\int_{\hat{y}_{\min}}^{\hat{y}_{\mathrm{dv}}} (2\hat{y})^\kappa f(\hat{y}) \mathrm{d}\hat{y}}_{=F(\theta_{\mathrm{dv}})} + \int_{\hat{y}_{\mathrm{dv}}}^{f^{-1}(\theta^{-1})} (2\hat{y})^\kappa f(\hat{y}) \mathrm{d}\hat{y} \quad (13)$$

Partial integration of the second integral in Eq. (13) gives

$$F(\theta) = F(\theta_{\mathrm{dv}}) + (2 f^{-1}(\theta^{-1}))^\kappa G(f^{-1}(\theta^{-1})) - (2\hat{y}_{\mathrm{dv}})^\kappa G(\hat{y}_{\mathrm{dv}}) - 2\kappa\left[H(f^{-1}(\theta^{-1})) - H(\hat{y}_{\mathrm{dv}}) \right] \quad (14)$$

The differential RTD for $\theta > \theta_{\mathrm{dv}}$ is given by Eq. (9). Eqs. (6), (9), (11), (12) and (14) are one of the main innovation of the present paper.

3. Pure convection RTDs for various velocity profiles

In this section we apply the theory from Section 2.2 to various velocity profiles. Amongst others, we consider three different generalized monotonic velocity profiles: generalized power law (which arises for Ostwald-de Waele power law fluids), generalized root law, and generalized film flow (which arises from Newtonian plane Couette-Poissueille flow). In Table 2 we list for each case the function $f(x)$ of the velocity profile, the inverse function f^{-1}, the derivative $f' = \mathrm{d}f/\mathrm{d}x$, and the anti-

derivatives $G = \int f \mathrm{d}x$ and $H = \int G \mathrm{d}x$, as well as θ_F, both for a planar channel and for a circular pipe. In all cases, f fulfills the normalization condition

$$\int_{\hat{y}_{\min}}^{1} (2\hat{y})^{\kappa} f(\hat{y}) \mathrm{d}\hat{y} = 1 \tag{15}$$

In the following subsections we derive the differential and cumulative RTD for the three mentioned generalized functions and some further velocity profiles. We start with pressure-driven flows in a circular pipe (Section 3.1), proceed with planar Couette and pressure-driven flows (Section 3.2) and finally consider the pressure-driven flow in a concentric annulus (Section 3.3).

3.1. Flows in a circular pipe

For the laminar flow in a circular pipe it is $\kappa = 1$, $\hat{y}_{\min} = 0$ and the velocity profile $u(\hat{r}) = U_\mathrm{m} f(\hat{r})$ is always monotonic. Then, Eqs. (9) and (6) become

$$E_\theta = -\frac{2}{\theta^3} \frac{f^{-1}(\theta^{-1})}{f'(f^{-1}(\theta^{-1}))} \tag{16}$$

$$F(\theta) = 2 f^{-1}(\theta^{-1}) G(f^{-1}(\theta^{-1})) - 2H(f^{-1}(\theta^{-1})) + 2H(0) \tag{17}$$

3.1.1. Ostwald-de Waele power law fluid in a pipe

In a circular pipe, the velocity profile of an Ostwald-de Waele power law fluid with flow behavior index n is given by $f(x) = \left(1 - x^{(n+1)/n}\right) / \theta_\mathrm{F}$ where $\theta_\mathrm{F} = U_\mathrm{m} / U_{\max} = (n+1)/(3n+1)$. The fluid is pseudoplastic for $n < 1$, is dilatant for $n > 1$, and is Newtonian for $n = 1$. With $f^{-1}(\theta^{-1}) = (1 - \theta_\mathrm{F}/\theta)^{n/(n+1)}$ and f' as given in Table 2, Eq. (16) yields

$$E_\theta = \frac{1}{\theta^3} \frac{2n}{3n+1} \left(1 - \frac{n+1}{3n+1} \frac{1}{\theta}\right)^{\frac{n-1}{n+1}} \tag{18}$$

This RTD was first derived by Foraboschi and Vaccari (1965) and Novosad and Ulbrecht (1966). Osborne (1975) and Garcia-Serna et al. (2007) also derived this RTD[1], however, represented it in terms of the *power law velocity profile index* $q = (n+1)/n$. For $0 < q \leq 2$ the differential RTD E_θ has a finite maximum at $\theta = 2(q+1)/3(q+2)$ while for $q > 2$ the maximum is infinite and located at $\theta_c = q/(q+2) = \theta_F$ (Osborne, 1975). For the cumulative RTD Eq. (17) yields

$$F = \left(1 + \frac{2n}{3n+1}\frac{1}{\theta}\right)\left(1 - \frac{n+1}{3n+1}\frac{1}{\theta}\right)^{\frac{2n}{n+1}} \tag{19}$$

in agreement with Cintron-Cordero et al. (1968). For $n = 1$ it is $\theta_F = 1/2$ and Eqs. (18) and (19) reduce to the well-known RTD of Newtonian pipe flow which was first obtained by Bosworth (1948) and is given by $E_\theta = 0.5\theta^{-3}$, $F = 1 - 0.25\theta^{-2}$.

3.1.2. Generalized root law velocity profile in a pipe

The velocity profile of the generalized rot law is $f(x) = (1-x)^{1/m}/\theta_F$ where we assume $m \geq 1$. For pipe flow it is $\theta_F = 2m^2(m+1)^{-1}(2m+1)^{-1}$. With $f^{-1}(\theta^{-1}) = 1 - (\theta_F/\theta)^m$ and f' as given in Table 2 we obtain from Eq. (16) the result

$$E_\theta = \frac{2m}{\theta_F^2}\left(\frac{\theta_F}{\theta}\right)^{m+2}\left[1 - \left(\frac{\theta_F}{\theta}\right)^m\right] \tag{20}$$

This RTD was first obtained by Bosworth (1949) as well. For the cumulative RTD Eq. (17) yields

$$F = 1 - \frac{2m+1}{m}\left(\frac{\theta_F}{\theta}\right)^{n+1}\left[1 - \frac{m+1}{2m+1}\left(\frac{\theta_F}{\theta}\right)^m\right] \tag{21}$$

3.1.3. Pipe flow of a Prandtl-Eyring fluid

The monotonic velocity profile of the flow of a Prandlt-Eyring fluid in a circular pipe is given by

[1] Note that in Osborne (1975) and Garcia-Serna et al. (2007) the symbol n is not the flow behavior index but the power law velocity profile index, which we here denote as q.

$$f\,(x) = \frac{1}{\theta_{\mathrm{F}}} \frac{\cosh(p) - \cosh(px)}{\cosh(p) - 1} \tag{22}$$

where

$$\theta_{\mathrm{F}} = \frac{\cosh(p)}{\cosh(p) - 1}\left[1 + \frac{2}{p^2}\left(1 - \frac{1 + p\sinh(p)}{\cosh(p)}\right)\right] \tag{23}$$

Here, p is a constant non-dimensional rheological parameter (Schenk and Van Laar, 1958); its effect on the velocity profiles is shown in Fig. 1 a). For $p = 1$ the velocity profile is close to that of Newtonian pipe flow whereas for $p = 100$ it approaches plug flow.

With the first derivative

$$f'(x) = -\frac{p}{\theta_{\mathrm{F}}} \frac{\sinh(px)}{\cosh(p) - 1}, \tag{24}$$

the inverse function

$$f^{-1}(x) = p^{-1} \cosh^{-1}\left[\cosh(p) - x\theta_{\mathrm{F}}\left(\cosh(p) - 1\right)\right], \tag{25}$$

and the antiderivatives

$$G(x) = \frac{1}{\theta_{\mathrm{F}}} \frac{x\cosh(p) - p^{-1}\sinh(px)}{\cosh(p) - 1}, \quad H(x) = \frac{1}{\theta_{\mathrm{F}}} \frac{\frac{1}{2}x^2\cosh(p) - p^{-2}\cosh(px)}{\cosh(p) - 1} \tag{26}$$

we obtain from Eqs. (16) and (17) the results

$$E_\theta = \frac{2\theta_{\mathrm{F}}}{\theta^3} \frac{\cosh(p) - 1}{p^2} \frac{\cosh^{-1}\left[\cosh(p) - \left(\cosh(p) - 1\right)\dfrac{\theta_{\mathrm{F}}}{\theta}\right]}{\sinh\left\{\cosh^{-1}\left[\cosh(p) - \left(\cosh(p) - 1\right)\dfrac{\theta_{\mathrm{F}}}{\theta}\right]\right\}} \tag{27}$$

$$F = \frac{1}{\theta_{\mathrm{F}}} \frac{1}{p^2} \frac{1}{\cosh(p) - 1}\left\{\Psi^2\cosh(p) - 2\Psi\sinh(\Psi) - 2\left[1 - \cosh(\Psi)\right]\right\} \tag{28}$$

where

$$\Psi = \cosh^{-1}\left[\cosh(p) - \left(\cosh(p) - 1\right)\frac{\theta_{\mathrm{F}}}{\theta}\right] \tag{29}$$

This RTD was first derived by Wein and Ulbrecht (1972). Fig. 1 b) illustrates the change of E_θ from Newtonian pipe flow toward plug flow as p is increased from 1 to 100.

3.2. Flows in a planar channel

For the laminar flow in a planar channel it is $\kappa = 0$, $\hat{y}_{\min} = 0$ and $u = U_{\mathrm{m}} f(\hat{y})$. If the velocity profile is monotonic, then Eq. (9) and Eq. (6) simplify to the form

$$E_\theta = -\frac{1}{\theta^3}\frac{1}{f'(f^{-1}(\theta^{-1}))} \tag{30}$$

$$F = G(f^{-1}(\theta^{-1})) - G(0) \tag{31}$$

For a non-monotonic velocity profile, Eq. (12) and Eq. (11) apply, and reduce to

$$E_\theta = -\frac{1}{\theta^3}\left(\frac{1}{f'(f_+^{-1}(\theta^{-1}))} - \frac{1}{f'(f_-^{-1}(\theta^{-1}))}\right) \tag{32}$$

$$F = G(f_+^{-1}(\theta^{-1})) - G(f_-^{-1}(\theta^{-1})) \tag{33}$$

3.2.1. Couette flow of Ostwald-de Waele power law fluid

The Couette flow velocity profile of an Ostwald-de Waele power law fluid with flow behavior index n is $f(x) = (1 - x^{(n+1)/n})/\theta_{\mathrm{F}}$, where $\theta_{\mathrm{F}} = (n+1)/(2n+1)$. With $f^{-1}(\theta^{-1}) = (1 - \theta_{\mathrm{F}}/\theta)^{n/(n+1)}$ Eqs. (30) and (31) become

$$E_\theta = \frac{1}{\theta^3}\frac{n}{2n+1}\left(1 - \frac{n+1}{2n+1}\frac{1}{\theta}\right)^{-\frac{1}{n+1}}, \qquad F = \left(1 - \frac{n+1}{2+1}\frac{1}{\theta}\right)^{\frac{n}{n+1}}\left(1 + \frac{n}{2n+1}\frac{1}{\theta}\right) \tag{34}$$

This RTD was first derived by Foraboschi and Vaccari (1965). For $n = 1$ we have $f(x) = (1 - x^2)/\theta_{\mathrm{F}}$ and $\theta_{\mathrm{F}} = 2/3$. This case corresponds to planar falling film flow and Eq. (34) yields the following results which were first obtained by Asbjornsen (1961)

$$E_\theta(\theta)=\frac{1}{3\theta^3}\left(1-\frac{2}{3\theta}\right)^{-\frac{1}{2}},\qquad F(\theta)=\left(1+\frac{1}{3\theta}\right)\left(1-\frac{2}{3\theta}\right)^{\frac{1}{2}} \tag{35}$$

In the limit $n\to\infty$ we have $f(x)=(1-x)/\theta_F$ and $\theta_F=1/2$. This case corresponds to planar Couette flow and Eq. (34) yields the same RTD as for Newtonian pipe flow (see above).

3.2.2. Planar Poiseuille flow

For planar Poiseuille flow it is $f(x)=4x(1-x)/\theta_F$ and $\theta_F=2/3$. With

$$f'(x)=\frac{4(1-2x)}{\theta_F},\qquad f_\pm^{-1}(x)=\frac{1}{2}\left(1\pm\sqrt{1-\theta_F x}\right) \tag{36}$$

Eqs. (32) and (33) become identical to the RTD of planar falling film flow, Eq. (35). This result is expected, because planar Poiseuille flow can be interpreted as consisting of two symmetric falling film flows which meet at the channel mid-plane (Levenspiel, 1989).

3.2.3. Falling film flow of a Prandtl-Eyring fluid

The monotonic velocity profile of the planar falling film flow of a Prandlt-Eyring fluid is given by Eq. (22). In the planar case, the non-dimensional first appearance time is

$$\theta_F=\frac{\cosh(p)-p^{-1}\sinh(p)}{\cosh(p)-1} \tag{37}$$

With the first derivative, Eq. (24), the inverse function, Eq. (25), the two antiderivatives, Eq. (26), the abbreviation

$$\Omega=\cosh(p)-\frac{p\cosh(p)-\sinh(p)}{p\theta} \tag{38}$$

and the identities $\sinh\left(\cosh^{-1}(\Omega)\right)=\sqrt{\Omega^2-1}$ and $\cosh^{-1}(\Omega)=\ln\left(\Omega+\sqrt{\Omega^2-1}\right)$ we obtain from Eqs. (30) and (31) the relations

$$E_\theta = \frac{1}{\theta^3}\frac{p\cosh(p)-\sinh(p)}{p^2\sqrt{\Omega^2-1}} \tag{39}$$

$$F = \frac{\cosh(p)\cdot\ln\left(\Omega+\sqrt{\Omega^2-1}\right)-\sqrt{\Omega^2-1}}{p\cosh(p)-\sinh(p)} \tag{40}$$

which were first derived by Sawinsky and Simandi (1983).

3.2.4. Plane Couette-Poiseuille flow of a Newtonian fluid

The velocity profile of plane Couette-Poiseuille flow of a Newtonian fluid can be found e.g. in Drazin and Riley (2006). In the terminology of the present paper, it is described by the function

$$f(x) = \frac{1}{\theta_{\mathrm{W}}}(1-x)(1+sx) \tag{41}$$

Here,

$$s = -\frac{H_{\|}^2}{2\mu U_{\mathrm{W}}}\frac{\partial p}{\partial z} \tag{42}$$

is a constant non-dimensional axial pressure gradient and $U_{\mathrm{W}} \geq 0$ is the velocity of the moving lower wall, while the upper wall is at rest. For $s = 0$ we have Couette flow, for $s = 1$ falling film flow (with a shear-free interface at $\hat{y} = 1$) and for $s \to \infty$ we have plane Poiseuille flow. In Eq. (41), $\theta_{\mathrm{W}} = (3+s)/6$ is the non-dimensional residence time that corresponds to the wall velocity U_{W}.

When s is in the range $0 \leq s \leq 1$, the velocity profile is monotonic and the inverse function is unique (see Table 2). The non-dimensional first appearance time is $\theta_{\mathrm{F}} = \theta_{\mathrm{W}}$. With the derivative f' given in Table 2 Eq. (30) becomes

$$E_\theta = \frac{\theta_{\mathrm{W}}}{\theta^3}\left[(1-s)^2 + 4s\left(1-\frac{\theta_{\mathrm{W}}}{\theta}\right)\right]^{-\frac{1}{2}} \tag{43}$$

This result was first obtained by Levenspiel et al. (1970)[2]. From Eq. (31) we obtain for the cumulative RTD after some tedious algebraic manipulations the result

$$F = 1 - \frac{1}{12\theta_W s^2}\left\{(1+s)^3 - \left[(1+s)^2 + 2s\frac{\theta_W}{\theta}\right]\sqrt{(1-s)^2 + 4s\left(1-\frac{\theta_W}{\theta}\right)}\right\} \tag{44}$$

For $s > 1$ the velocity profile is not monotonic, see Fig. 2 a). The velocity maximum is located at $(s-1)/(2s)$ and the corresponding value of the first appearance time is $\theta_F = (2s/3)(3+s)/(1+s)^2 = 4s\theta_W/(1+s)^2$. For $\hat{y} > \hat{y}_{dv} = (s-1)/s$ the inverse function is single-valued and the same as given in Table 2. For $\hat{y} \le \hat{y}_{dv}$ the inverse function has two branches:

$$f_{\pm}^{-1}(x) = \frac{(s-1) \pm \sqrt{(s-1)^2 + 4s(1-\theta_W x)}}{2s} \tag{45}$$

By the theory in the second paragraph of Section 2.2.2 we obtain for the differential RTD the result

$$E_\theta = \begin{cases} \dfrac{2\theta_W}{\theta^3}\left[(1-s)^2 + 4s\left(1-\dfrac{\theta_W}{\theta}\right)\right]^{-\frac{1}{2}} & \dfrac{4s}{(1+s)^2}\theta_W \le \theta \le \theta_W \\ \dfrac{\theta_W}{\theta^3}\left[(1-s)^2 + 4s\left(1-\dfrac{\theta_W}{\theta}\right)\right]^{-\frac{1}{2}} & \theta > \theta_W = \dfrac{3+s}{6} \end{cases} \tag{46}$$

This RTD is derived here for the first time. It is displayed in Fig. 2 b) for four different values of s and has two interesting features. First, it is discontinuous at θ_W where it decreases by a factor of two. While this behavior is at first surprising, it is reasonable since for $\theta < \theta_W$ there are two lateral locations within the channel with a given residence time, whereas for $\theta > \theta_W$ it is only one. This explains the sudden decrease of E_θ by a factor of two at $\theta = \theta_W$. The second notable feature of this RTD is the non-monotonic dependence of its first appearance time on s. For $s = 1$ and $s \to \infty$ we have $\theta_F = 2/3$ while for $1 < s < \infty$ we have $\theta_F > 2/3$. The maximum value $\theta_F = 0.75$ is obtained for $s = 3$. This result has some practical implications for tracers with high Schmidt number in plane Couette-Poiseuille flow

[2] Note that in their nomenclature it is $s = 1 - \beta$.

of Newtonian liquids. It suggest that in order to achieve a narrow residence time distribution (which is usually wanted in practice), s should be close to 3. From Eq. (42) we can then directly determine the optimal value of the axial pressure drop which minimizes the width of the RTD, and the corresponding optimal value of the volumetric flow per unit depth which is $Q_{\text{total}} = H_{\|} U_{\text{W}}$.

3.2.5. Generalized root law velocity profile in a planar channel

For the planar case, the non-dimensional first appearance time of the generalized root velocity profile from Section 3.1.2 is given by $\theta_{\text{F}} = m/(m+1)$. With $f^{-1}(\theta^{-1}) = 1-(\theta_{\text{F}}/\theta)^m$ we obtain from Eqs. (30) and (31) the results

$$E_\theta = \frac{m\theta_{\text{F}}^m}{\theta^{m+2}} = \frac{m^{m+1}}{(m+1)^m}\frac{1}{\theta^{m+2}}, \qquad F = 1-\left(\frac{m}{m+1}\frac{1}{\theta}\right)^{m+1} \tag{47}$$

To our knowledge, also this RTD has not been derived before.

3.3. Flow in a concentric annulus

As final example we consider the flow of a Newtonian fluid in an annulus formed by two concentric cylinders. The velocity profile $u = U_{\text{m}} f(\hat{r})$ in the range $\alpha \le \hat{r} \le 1$ is given by

$$f(x) = \frac{1}{\theta_{\text{F}}}\frac{1-x^2+2\lambda^2\ln x}{1-\lambda^2+2\lambda^2\ln\lambda} \tag{48}$$

The first appearance time is

$$\theta_{\text{F}}(\alpha) = \frac{1}{2}\frac{1+\alpha^2-2\lambda^2}{1-\lambda^2+2\lambda^2\ln\lambda} \tag{49}$$

where

$$\lambda(\alpha) = \sqrt{\frac{1-\alpha^2}{2\ln\alpha^{-1}}} \tag{50}$$

is the non-dimensional radial position of the maximum velocity (Nigam and Vasudeva, 1976). The first derivative and the inverse function are given by

$$f'(x)=\frac{1}{\theta_F}\frac{-2x+2\lambda^2x^{-1}}{1-\lambda^2+2\lambda^2\ln\lambda},\quad f_{\pm}^{-1}(x)=\lambda\sqrt{-W_{\pm}\left(-\frac{1}{\lambda^2}\exp\left(-\frac{1}{\lambda^2}+\frac{x\theta_F(1-\lambda^2+2\lambda^2\ln\lambda)}{\lambda^2}\right)\right)} \tag{51}$$

Here, $W_+(x)=W_0(x)$ and $W_-(x)=W_{-1}(x)$ are the lower and upper branch of the Lambert W-function (Golicnik, 2012; Veberic, 2012; Williams, 2010), where the argument is in the range $-e^{-1}\le x<0$. With the latter equations and $\kappa=1$, the RTD can be expressed via Eq. (12) in the following closed analytical form

$$E_\theta=\frac{1}{2\theta^3}\left(1+\alpha^2-\frac{1-\alpha^2}{\ln\alpha^{-1}}\right)\frac{W_0(\beta)-W_{-1}(\beta)}{\left(1+W_0(\beta)\right)\left(1+W_{-1}(\beta)\right)} \tag{52}$$

where

$$\beta=-\frac{1}{\lambda^2}\exp\left(-\frac{1}{\lambda^2}+\frac{\theta_F}{\theta}\frac{1-\lambda^2+2\lambda^2\ln\lambda}{\lambda^2}\right) \tag{53}$$

Nigam and Vasudeva (1976) where the first who derived this RTD; however, they gave it only in implicit form and their Eq. (11) for F contains two errors. The RTD of annular flow is similar to that of flow between parallel plates except when α is very small (Nauman and Buffham, 1983). We remark that the RTD given by Foraboschi and Vaccari (1965) for the flow of a Newtonian liquid in an annulus is incorrect, as noted by Pechoč (1983).

Lin (1980) determined the RTD of an Ostwald-de Waele power law fluid in a concentric annulus analytically on basis of the approximate velocity profile of Mishra and Mishra (1976). Pechoč (1983) evaluated the RTD numerically from the exact velocity profile and showed that the approximate results of Lin (1980) differ significantly from the exact ones only in the vicinity of θ_F.

3.4. Further non-Newtonian velocity profiles

In literature the diffusion-free RTD of fully developed laminar flow in a circular pipe has been derived for further generalized velocity profiles (Pegoraro et al., 2012) as well as for further non-Newtonian fluids. The latter encompass Herschel-Bulkley fluids (Delaplace et al., 2008; Sawinsky and Deak, 1995; Wein and Ulbrecht, 1972), Bingham and Rabinowitsch fluids (Wein and Ulbrecht, 1972)

and Cassonian fluids (Sawinsky and Balint, 1984). The RTD of a Bingham fluid in a planar falling film was derived by Zakharov (2006). We expect that all these RTDs are recovered from the present theory as well, though we have not explicitly checked this for all these velocity profiles.

4. Discussion

In this section we use Eq. (9) to investigate certain properties of the differential RTD of diffusion-free fully developed laminar flow. In particular we investigate (i) the asymptotic behavior of the RTD for large values of θ, (ii) the variance of the RTD and (iii) the effect of a finite wall velocity.

4.1. Asymptotic behavior of the RTD

Large values of the residence time correspond to low velocities. The lowest velocities and, therefore, the largest residence times occur in the vicinity of the wall (or more generally the domain boundary where $u = U_{\min}$). The corresponding upper limit of the dimensionless residence time is $\theta_{\max} = U_{\mathrm{m}} / U_{\min}$. For any viscous flow, there exists a sublayer of thickness δ in the immediate vicinity of a no-slip wall (which may be either stationary or moving with a finite velocity) where the fluid velocity increases linearly with the wall distance so that $a = \left(-\mathrm{d}\hat{u} / \mathrm{d}\hat{y}\right)\big|_{\hat{y}=1}$. Thus, for $a \neq 0$ there is an interval $x \in [1-\delta, 1]$ where $f(x) = a(1-x) + 1/\theta_{\max}$ so that $f^{-1}(x) = 1 - (x - 1/\theta_{\max})/a$ and $f' = -a = const$. Introducing these relations into Eq. (9) yields

$$E_\theta = \frac{1}{a\theta^3}\left[2 - \frac{2}{a}\left(\frac{1}{\theta} - \frac{1}{\theta_{\max}}\right)\right]^\kappa \tag{54}$$

so that

$$\lim_{\theta \to \theta_{\max}} E_\theta = \frac{2^\kappa}{a}\frac{1}{\theta^3} \tag{55}$$

By Eq. (55) we have shown that for any laminar velocity profile in a duct with a no-slip condition at a stationary or moving wall and a linear slope $a \neq 0$ the asymptotic behavior of the diffusion-free

differential RTD follows a θ^{-3} power law. This asymptotic behavior was already shown by Wein and Ulbrecht (1972) for the special case of a circular pipe and a stationary no-slip wall. In fact, for $\kappa = 1$ and $\theta_{\max} \to \infty$ the present Eq. (55) reduces to Eq. (42a) in Wein and Ulbrecht (1972). By integration of Eq. (55) we find for the asymptotic behavior of the cumulative RTD the relation

$$\lim_{\theta \to \theta_{\max}} F(\theta) = 1 - \frac{2^{\kappa-1}}{a} \frac{1}{\theta^2} \tag{56}$$

This result is in accordance with the theoretical considerations of Nauman (1977) on generalized flow situations with a stationary wall. In the absence of molecular diffusion he found for the cumulative RTD in the limit $\theta \to \infty$ the asymptotic behavior $F(\theta) = 1 - \gamma / \theta^2$, where γ is a constant. Here, we determined the value of this constant as $2^{\kappa-1} / a$ and demonstrated that this asymptotic behavior is not limited to no-slip conditions at stationary walls but applies to moving walls as well.

To illustrate the asymptotic -3 power law behavior of the differential RTD, we display in Fig. 3 a) and b) the term $\theta^3 E_\theta$ for the generalized power law velocity profile in a circular pipe and in a planar channel for different values of parameter q. From this figure it is evident, that $\theta^3 E_\theta$ becomes indeed independent of θ for large residence times. The respective constant value is in all cases consistent with Eq. (55).

In Fig. 3 c) we show the term $\theta^3 E_\theta$ versus θ for the generalized root law velocity profile in a planar channel. It is interesting to note that the asymptotic behavior of this RTD does *not* follow a -3 power law for $m > 1$. Instead $\theta^3 E_\theta$ approaches zero for large values of θ. This also holds for the generalized root law velocity profile in a circular pipe not shown here. The reason for this different asymptotic behavior stems from the fact that for the generalized root velocity profile it is $a = \left(-\mathrm{d}\hat{u} / \mathrm{d}y\right)\Big|_{y=1} = 0$ for $m > 1$, i.e. this velocity profile does not show the linear increase of the velocity with the wall distance which is in reality characteristic for viscous laminar flows.

4.2. Variance of the RTD

In this subsection we investigate the implications of the above theory for the variance of the RTD. Sawinsky and Balint (1984) remarked that in the case of pure laminar flow with no molecular diffusion the concept of variance of the RTD has no meaning. They argued that the variance it a statistical quantity, which gives the mean square deviation from the statistical mean values. The variance has a meaning only when the distribution is of a statistical nature. This is not the case for laminar flows with no molecular diffusion, where the RTD is fully deterministic. Also Nauman (2004) noted that the dimensionless variance has limited usefulness in laminar flow systems. In the present context the variance of the RTD is, nevertheless, of some theoretical interest.

The definition of the variance σ_θ^2 is given in Eq. (2). Whether the variance of an RTD is finite or infinite depends on the tail of the RTD, i.e. the asymptotic behavior of the RTD as θ approaches infinity (cf. section 4.1). Nauman (1977) noted that the asymptotic behavior $F(\theta) = 1 - \gamma / \theta^2$ implies that – were it not for diffusion – all residence time distributions would have an infinite variance.

Here, we consider as an example the general monotonic velocity profile of section 2.2.1 for the planar case ($\kappa = 0$). By expansion of the quadratic term in Eq. (2), by taking into account Eq. (1) and by introducing these expressions into Eq. (9) it follows

$$\sigma_\theta^2 = -1 + \int_{\theta_F}^{\infty} \theta^2 E_\theta \, \mathrm{d}\theta = -1 - \int_{\theta_F}^{\infty} \frac{1}{\theta} \frac{1}{f'(f^{-1}(\theta^{-1}))} \mathrm{d}\theta \tag{57}$$

Whether the integral in Eq. (57) converges or not depends on the behavior of the integrand in the limit $\theta \to \infty$. This limit is equivalent to $\hat{u} = 1/\theta \to 0$, i.e. the behavior of the normalized velocity profile at a stationary no-slip wall. For the generic monotonic laminar velocity profile of Section 2.2.1, the solid wall is located at $\hat{y} = 1$ and it is $\hat{u}_{\hat{y}\to 1} = f_{\text{asymptotic}}(\hat{y}) = a(1-\hat{y})$ with the wall velocity gradient $a > 0$. Then it is $f'_{\text{asymptotic}} = -a$ so that Eq. (57) becomes

$$\sigma^2 = -1 - \int_{\theta_F}^{\theta_{asymtotic}} \frac{1}{\theta} \frac{1}{f'(f^{-1}(\theta^{-1}))} \mathrm{d}\theta + \int_{\theta_{asymtotic}}^{\infty} \frac{1}{a\theta} \mathrm{d}\theta \tag{58}$$

While the value of the first integral in Eq. (58) is finite, that of the second integral is infinite so that $\sigma^2 = \infty$. A similar analysis can be done for general non-monotonic velocity profiles and the case $\kappa = 1$. This result suggests that for diffusion-free laminar flows with a stationary no-slip wall the variance of the RTD and any moment higher than one is infinite.

Indeed, evaluation of Eq. (2) for the diffusion-free RTDs of the various velocity profiles from Section 3 confirms that σ_θ^2 is infinite, with one notable exception. Namely, for the RTDs of the generalized root velocity profile the variance is finite. For the circular pipe RTD, Eq. (20), we obtain

$$\sigma_\theta^2 = \frac{4m^2(7m^2-1)}{(m-1)(m+1)^2(2m-1)(2m+1)^2} \tag{59}$$

while for the planar channel RTD, Eq. (47), it is

$$\sigma_\theta^2 = \frac{2m}{(m-1)(m+1)^2} \tag{60}$$

These finite values of the variance for $m > 1$ are related to the fact that for the root law velocity profile it is $a = 0$ so that $\theta^3 E_\theta$ does not approach asymptotically a finite constant value but zero instead (cf. Fig. 3 c).

4.3. Effect of finite wall velocity

While the results in the previous section apply to velocity profiles which are zero at the wall, we extend our analysis in this section to laminar flows where the fluid velocity at the wall is finite. Typical examples are flows where the wall is moving and electro-osmotic flows where both, an applied pressure gradient and an external electric field drive the flow. In the latter case the charge on the wall leads to a finite velocity of the electrolyte within the electric double-layer close to the wall. Hsu and Wei (2005) studied the influence of the electric field and double layer thickness on the RTD in a cylindrical micro-reactor numerically and showed that this technique can be used to narrow the RTD.

To study the effect of a finite wall velocity on the RTD we consider a planar channel where the lower and upper wall move with velocity $U_{\max}$ and $U_{\min} = \psi U_{\max}$, respectively, where $0 \le \psi < 1$. The linear velocity profile is

$$f(x) = \frac{1-(1-\psi)x}{\theta_F} \tag{61}$$

where $\theta_F = (1+\psi)/2$. The value $\psi = 0$ corresponds to plane Couette flow (see Section 3.2.1) and the limit $\psi \to 1$ to plug flow. With $f' = -(1-\psi)/\theta_F$ we obtain from Eq. (30) the result

$$E_\theta = \begin{cases} \dfrac{1}{1-\psi}\dfrac{\theta_F}{\theta^3} & \theta_F \le \theta \le \theta_F/\psi \\ 0 & \text{otherwise} \end{cases} \tag{62}$$

The variance of this RTD is

$$\sigma_\theta^2 = \int_{\theta_F}^{\theta_F/\psi} \frac{(\theta-1)^2}{1-\psi}\frac{\theta_F}{\theta^3}\mathrm{d}\theta = -1 - \frac{1}{2}\frac{1+\psi}{1-\psi}\ln\psi \tag{63}$$

This relation is displayed in Fig. 4. The variance according to Eq. (63) is finite for $0 < \psi < 1$, whereas it is infinite in the limit $\psi \to 0$, i.e. for a stationary no-slip wall. In the limit $\psi \to 1$ the velocity profile approaches plug flow and the variance becomes zero.

5. Conclusions

In this paper general mathematical expressions have been derived which allow computing the diffusion-free differential and cumulative RTD of a given one-dimensional velocity profile. These relations are useful to compute the convection model RTD of fully developed laminar flow in straight planar and axisymmetric ducts. The present theory is unifying in the sense that it should include all convection model RTDs published in literature so far. This has been demonstrated for a number of Newtonian, non-Newtonian and generalized velocity profiles in a planar channel or film, in a circular pipe and in a concentric annulus, which were derived in previous literature on a case-by-case basis.

The theory is used to derive some convection model RTDs for velocity profiles or geometries that have not been obtained before. Most notable is the differential RTD of Newtonian plane Couette-Poiseuille flow with non-monotonic velocity profile, which is found to be discontinuous at that value of the residence time which corresponds to the moving wall velocity. The optimum flow rate where the residence time distribution is most narrow is also determined.

The general mathematical expression for the non-dimensional differential RTD is used to study the asymptotic behavior of the RTD in the limit of large residence times. It is demonstrated that any one-dimensional velocity profile which shows a linear dependence on the distance from a stationary or moving no-slip wall results in a diffusion-free RTD which follows an asymptotic -3 power law. This has implications for general laminar *and* turbulent flow systems. Since any viscous fluid flow possesses a laminar sublayer, where the axial velocity increases linearly with the wall distance, the pure convection RTD of any real viscous flow system should show this asymptotic -3 power law behavior of the differential RTD. This finding is consistent with the respective -2 power law of the diffusion-free cumulative RTD of general flow systems proposed by Nauman (1977). Closely related to the asymptotic behavior of the RTD is the variance of the RTD. For the asymptotic -3 power law behavior, the variance is shown to be infinite for a stationary wall and finite for a moving wall.

At this stage, the present mathematical analysis on the pure convection RTD of laminar flows is mainly of theoretical and scientific interest, since in practice diffusion is always present. For liquid flows in micro-channels, the diffusivity is very small (high Schmidt number) and there are situations where the effect of diffusion on the RTD is limited to regions close to the channel walls (where the residence time is very large), while convection governs the RTD in the channel center (where the residence time is low). At present, there exist to our knowledge no suitable and predictive models to describe such RTDs. We now work on combing the present pure convective RTD theory with near wall diffusion effects, in order to develop a model which is also of some practical relevance for certain situations. A key parameter in this model will be the “critical” residence time θ_c above which diffusion becomes important as it changes the asymptotic behavior (“tailing”) of the RTD and making the

variance finite. The present theory suggests, that one can estimate this critical residence time θ_c by displaying $\theta^3 E_\theta$ versus θ, cf. Fig. 1. In a semi-logarithmic plot, $\theta^3 E_\theta$ should exhibit - at sufficient large values of θ - a range where the curve is about constant ($\theta < \theta_c$) before it decays to zero ($\theta > \theta_c$).

Notation

A	area of channel cross section, m^2
a	gradient of velocity profile at the wall, dimensionless
E_θ	differential RTD function, dimensionless
f	function describing the one-dimensional velocity profile, dimensionless
f^{-1}	inverse function of f, dimensionless
f'	derivative of function f, dimensionless
F	cumulative RTD function, dimensionless
G	antiderivative of function f, dimensionless
H	antiderivative of function G, dimensionless
$H_{\|\|}$	height of planar channel or film, m
L	channel length, m
m	parameter in generalized root law velocity profile, dimensionless
n	flow behavior index of Ostwald-de Waele fluid, dimensionless
p	rheological parameter of Prandtl-Eyring fluid, dimensionless
q	parameter in generalized power law velocity profile, $q = (n+1)/n$, dimensionless
Q	volumetric flow rate, m^3/s
Q_{total}	total volumetric flow rate, m^3/s
r	radial co-ordinate in pipe and annulus, m
$\hat{r} = r / R$	normalized radial co-ordinate in pipe and annulus, dimensionless
R	radius of pipe or outer radius of annulus, m
s	parameter in plane Couette-Poiseuille flow velocity profile, dimensionless
t	time, s

t_{m}	mean residence time, s
u	profile of axial velocity, m/s
$\hat{u} = u / U_{\mathrm{m}}$	normalized profile of axial velocity, dimensionless
$U_{\max}$	maximum velocity of profile u, m/s
$U_{\min}$	minimum velocity of profile u, m/s
U_{m}	mean velocity, m/s
V	volume of flow domain, m^3
W_+, W_-	upper and lower branch of Lambert W-function, dimensionless
x	argument of function f, dimensionless
y	wall-normal (lateral) co-ordinate, m
$\hat{y}$	normalized wall-normal (lateral) co-ordinate, dimensionless

Greek letters

α	ratio of inner to outer diameter of concentric annulus, dimensionless
β	expression in RTD of concentric annulus, dimensionless
δ	thickness of viscous sublayer, m
θ	normalized residence time, dimensionless
θ_{F}	first appearance time, dimensionless
θ_{W}	residence time corresponding to wall velocity in Couette-Poiseuille flow, dimensionless
κ	geometry parameter, dimensionless
λ	radial position of maximum velocity in annulus, dimensionless
μ_0, μ_1	zero and first moment of differential RTD, dimensionless
σ_θ^2	variance of differential RTD, dimensionless
ψ	ratio between mean and maximum velocity, dimensionless

References

Asbjornsen, O.A., 1961. The Distribution of Residence Times in a Falling Water Film. Chemical Engineering Science 14, 211-227.

Bosworth, R.C.L., 1948. Distribution of reaction times for laminar flow in cylindrical reactors. Philosophical Magazine Series 7 39, 847-862.

Bosworth, R.C.L., 1949. Distribution of reaction times for turbulent flow in cylindrical reactors. Philosophical Magazine Series 7 40, 314-324.

Cantu-Perez, A., Barrass, S., Gavriilidis, A., 2010. Residence time distributions in microchannels: Comparison between channels with herringbone structures and a rectangular channel. Chemical Engineering Journal 160, 834-844.

Cintron-Cordero, R., Mostello, R.A., Biesenberger, J.A., 1968. Reactor Dynamics and Molecular Weight Distributions - Some Aspects of Continuous Polymerization in Tubular Reactors. Canadian Journal of Chemical Engineering 46, 434-443.

Danckwerts, P.V., 1953. Continuous Flow Systems - Distribution of Residence Times. Chemical Engineering Science 2, 1-13.

Danckwerts, P.V., 1958. The Effect of Incomplete Mixing on Homogeneous Reactions. Chemical Engineering Science 8, 93-102.

Delaplace, G., Thakur, R.K., Bouvier, L., Lepretre, C., Llnyzckyj, C., Andre, C., Nouar, C., 2008. Influence of rheological behavior of purely viscous fluids on analytical residence time distribution in straight tubes. Chemical Engineering & Technology 31, 231-236.

Drazin, P.G., Riley, N., 2006. The Navier-Stokes equations: a classification of flows and exact solutions. Cambridge University Press, Cambridge, UK; New York.

Erdogan, S., Wörner, M., 2013. Influence of channel cross-sectional shape on diffusion-free residence time distribution in fully developed laminar Newtonian flow. Chemical Engineering Journal 227, 158-165.

Fogler, H.S., 1986. Elements of chemical reaction engineering. Prentice-Hall, Englewood Cliffs, NJ.

Foraboschi, F.P., Vaccari, A., 1965. La Distribuzione Dei Tempi Di Permanenza Nei Fluidi in Moto Laminare. Ingegneria Chimica Italiana 1, 144-149.

Garcia-Serna, J., Garcia-Verdugo, E., Hyde, J.R., Fraga-Dubreuil, J., Yan, C., Poliakoff, M., Cocero, M.J., 2007. Modelling residence time distribution in chemical reactors: A novel generalised n-laminar model - Application to supercritical CO2 and subcritical water tubular reactors. Journal of Supercritical Fluids 41, 82-91.

Gogos, C.G., Tadmor, Z., Kalyon, D.M., Hold, P., Biesenberger, J.A., 1987. Polymer Processing - an Overview. Chemical Engineering Progress 83, 33-58.

Golicnik, M., 2012. On the Lambert W function and its utility in biochemical kinetics. Biochemical Engineering Journal 63, 116-123.

Ham, J.H., Lohse, R., Platzer, B., 2011. Modeling of the Laminar Flow in the Entrance Region of Tubes and Ducts and its Impact on the Residence Time Distribution. Chemie Ingenieur Technik 83, 1245-1255.

Hsu, J.P., Wei, T.H., 2005. Residence time distribution of a cylindrical microreactor. Journal of Physical Chemistry B 109, 9160-9165.

Kockmann, N., 2006. Micro process engineering: fundamentals, devices, fabrication, and applications. Wiley-VCH, Weinheim.

Levenspiel, O., 1989. The chemical reactor omnibook, 2nd ed. Oregon State University Book Stores.

Levenspiel, O., 1999. Chemical reaction engineering, 3rd ed. John Wiley & Sons, Hoboken, NJ.

Levenspiel, O., Lai, B.W., Chatlynne, C.Y., 1970. Tracer curves and the residence time distribution. Chemical Engineering Science 25, 1611-1613.

Lin, S.H., 1980. The Residence Time Distribution for Laminar Non-Newtonian Flow in an Annulus with Negligible Diffusion. Chemical Engineering Science 35, 1477-1480.

Lohse, S., Kohnen, B.T., Janasek, D., Dittrich, P.S., Franzke, J., Agar, D.W., 2008. A novel method for determining residence time distribution in intricately structured microreactors. Lab on a Chip 8, 431-438.

Madeira, L.M., Mendes, A., Magalhaes, F.D., 2006. Teaching Laminar-flow reactors: From experimentation to CFD simulation. International Journal of Engineering Education 22, 188-196.

Mishra, P., Mishra, I., 1976. Flow Behavior of Power Law Fluids in an Annulus. AIChE Journal 22, 617-619.

Nauman, E.B., 1974. Mixing in Polymer Reactors. Journal of Macromolecular Science, Part C 10, 75-112.

Nauman, E.B., 1977. Residence Time Distribution for Laminar-Flow in Helically Coiled Tubes. Chemical Engineering Science 32, 287-293.

Nauman, E.B., 2004. Residence time distributions, in: Paul, E.L., Atiemo-Obeng, V.A., Kresta, S.M. (Eds.), Handbook of industrial mixing: science and practice. Wiley-Interscience, Hoboken, N.J., pp. 1-17.

Nauman, E.B., Buffham, B.A., 1983. Mixing in continuous flow systems. Wiley, New York ; Chichester.

Nigam, K.D.P., Vasudeva, K., 1976. Studies on Tubular Flow Reactor with Motionless Mixing Elements. Industrial & Engineering Chemistry Process Design and Development 15, 473-476.

Novosad, Z., Ulbrecht, J., 1966. Conversion in Chemical Reactions for Isothermal Laminar Flow of Non-Newtonian Liquids in a Tubular Reactor of Circular Cross-Section. Chemical Engineering Science 21, 405-411.

Osborne, F.T., 1975. Purely Convective Models for Tubular Reactors with Non-Newtonian Flow. Chemical Engineering Science 30, 159-166.

Pechoc, V., 1983. The Residence Time Distribution for Laminar-Flow in an Annulus with Negligible Diffusion. Chemical Engineering Science 38, 1341-1342.

Pegoraro, P.R., Marangoni, M., Gut, J.A.W., 2012. Residence Time Distribution Models Derived from Non-Ideal Laminar Velocity Profiles in Tubes. Chemical Engineering & Technology 35, 1593-1603.

Sawinsky, J., Balint, A., 1984. The Residence Time Distribution for Laminar-Flow of a Cassonian Fluid in a Straight Circular Tube. Acta Chimica Hungarica-Models in Chemistry 117, 263-269.

Sawinsky, J., Deak, A., 1995. Residence Time Distribution for Laminar-Flow of a Herschel-Bulkley Fluid in a Straight Circular Tube. Magyar Kemiai Folyoirat 101, 293-295.

Sawinsky, J., Simandi, B., 1983. Residence Time Distribution for the Laminar Falling Film of a Prandtl-Eyring Liquid. Acta Chimica Hungarica-Models in Chemistry 112, 469-475.

Schenk, J., Van Laar, J., 1958. Heat transfer in non-Newtonian laminar flow in tubes. Applied Scientific Research, Section A 7, 449-462.

Torres, A.P., Oliveira, F.A.R., 1998. Residence time distribution studies in continuous thermal processing of liquid foods: a review. Journal of Food Engineering 36, 1-30.

Veberic, D., 2012. Lambert W function for applications in physics. Computer Physics Communications 183, 2622-2628.

Vikhansky, A., 2011. Numerical analysis of residence time distribution in microchannels. Chemical Engineering Research & Design 89, 347-351.

Wein, O., Ulbrecht, J., 1972. Residence time distribution in laminar flow systems. II: Non-Newtonian tubular flow. Collection of Czechoslovak Chemical Communications 37, 3240-3259.

Wibel, W., Wenka, A., Brandner, J.J., Dittmeyer, R., 2013. Measuring and modeling the residence time distribution of gas flows in multichannel microreactors. Chemical Engineering Journal 215, 449-460.

Williams, B.W., 2010. The Utility of the Lambert Function W[a exp(a-bt)] in Chemical Kinetics. Journal of Chemical Education 87, 647-651.

Wörner, M., 2010. Approximate residence time distribution of fully develop laminar flow in a straight rectangular channel. Chemical Engineering Science 65, 3499-3507.

Zakharov, M.K., 2006. Analysis of the flow pattern in apparatuses with laminar flows of non-Newtonian fluids. Theoretical Foundations of Chemical Engineering 40, 319-324.

Zwietering, T.N., 1959. The Degree of Mixing in Continuous Flow Systems. Chemical Engineering Science 11, 1-15.

Figure captions

Fig. 1: Velocity profile (a) and differential RTD (b) of a Prandtl-Eyring fluid flowing in a circular pipe for four different values of the non-dimensional rheological parameter p (solid lines). The dashed and dotted lines in both figures correspond to the velocity profile and RTD of Newtonian pipe flow and plug flow, respectively.

Fig. 2: Velocity profile (a) and differential RTD (b) of plane Couette-Poiseuille flow of a Newtonian fluid for different values of the non-dimensional pressure drop parameter s.

Fig. 3: Asymptotic behavior of the differential RTD of the generalized power law velocity profile in a circular pipe (a) and a planar channel (b), and of the generalized root law velocity profile in a planar channel (c).

Fig. 4: Variance of the RTD of planar channel flow as function of $\psi = U_{\min} / U_{\max}$.

Figures

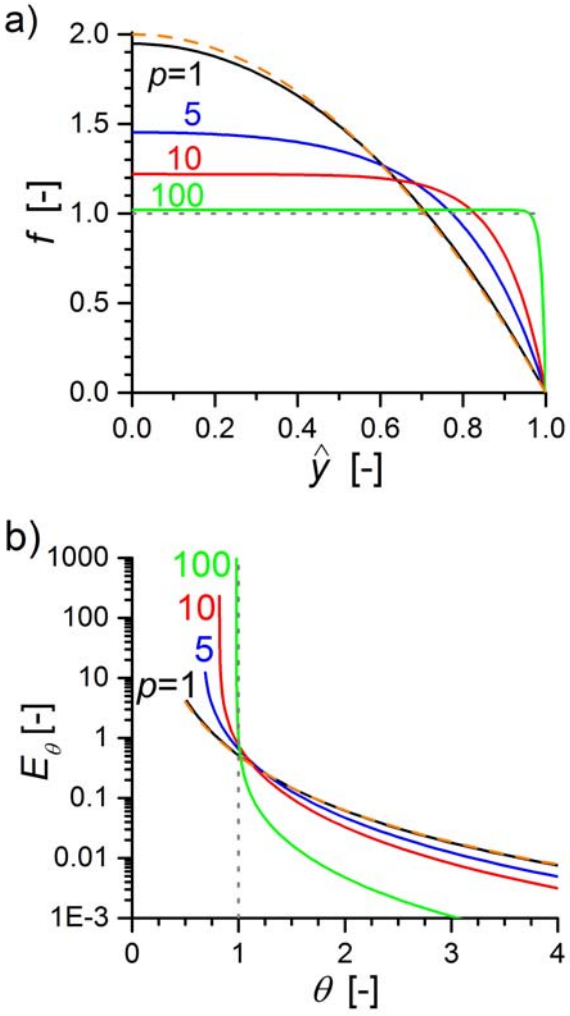

Fig. 1: Velocity profile (a) and differential RTD (b) of a Prandtl-Eyring fluid flowing in a circular pipe for four different values of the non-dimensional rheological parameter p (solid lines). The dashed and dotted lines in both figures correspond to the velocity profile and RTD of Newtonian pipe flow and plug flow, respectively.

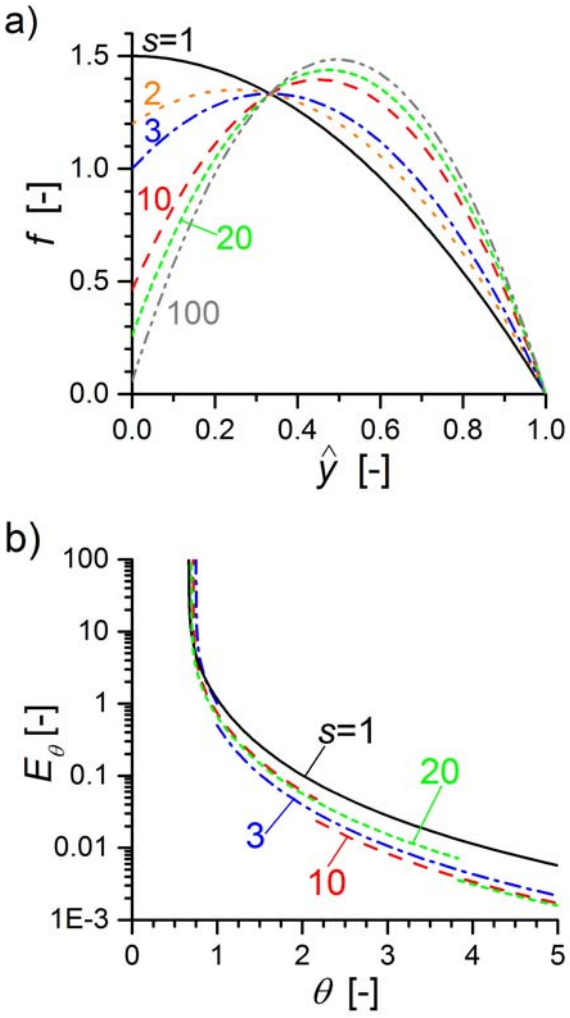

Fig. 2: Velocity profile (a) and differential RTD (b) of plane Couette-Poiseuille flow of a Newtonian fluid for different values of the non-dimensional pressure drop parameter s.

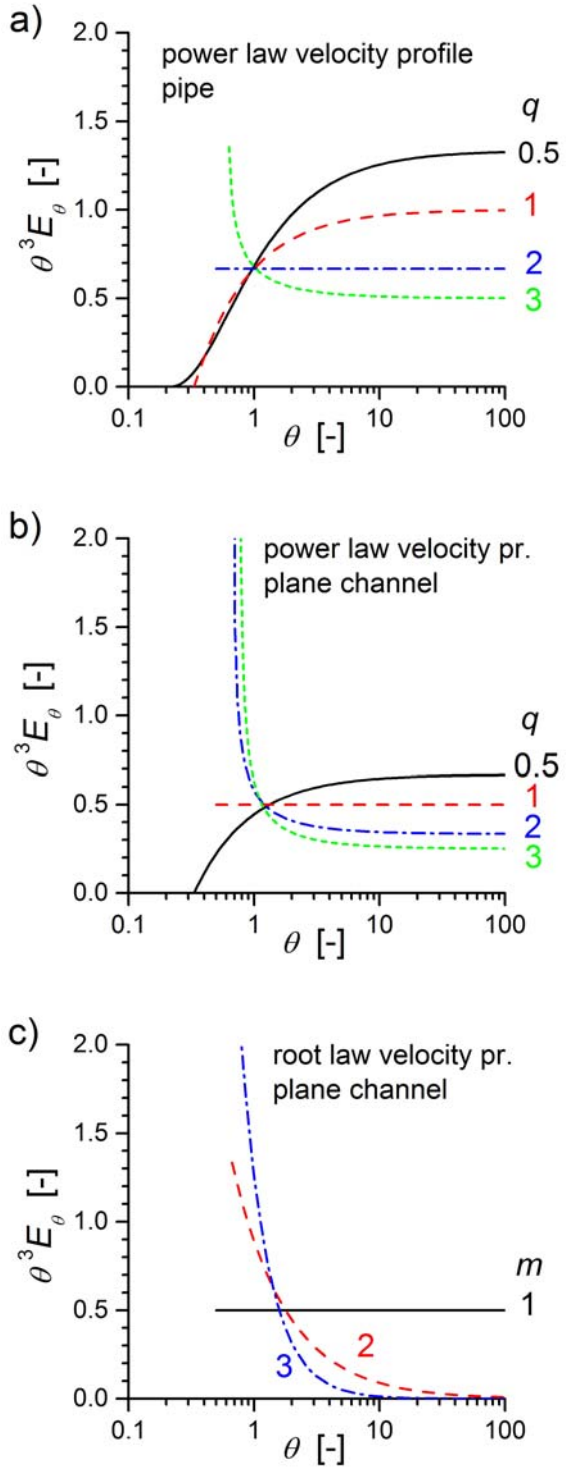

Fig. 3: Asymptotic behavior of the differential RTD of the generalized power law velocity profile in a circular pipe (a) and a planar channel (b), and of the generalized root law velocity profile in a planar channel (c).

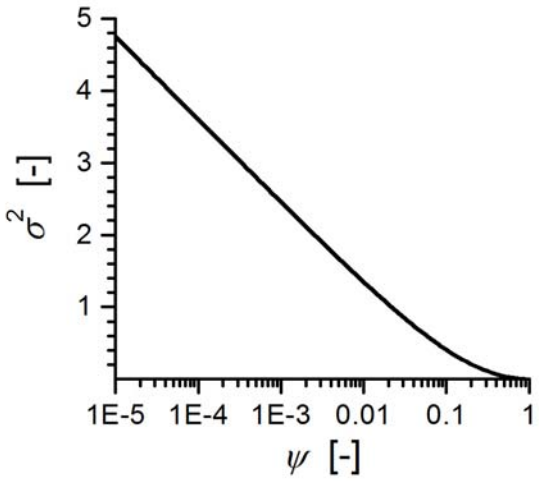

Fig. 4: Variance of the RTD of planar channel flow as function of $\psi = U_{\min} / U_{\max}$.

Tables

Table 1: Overview on pure convection RTDs for one-dimensional velocity profiles derived in previous literature for different fluids and flow type/driving-force (C = Couette flow, E = electro-osmotic driven, F = falling film flow, G = generalized velocity profile, P = pressure-driven flow). RTDs which are first derived in the present paper are also included.

Geometry	Fluid/velocity profile	Flow type	Reference
Planar	Newtonian	C	Levenspiel et al. (1970)
	"	F	Asbjornsen (1961)
	"	P	Levenspiel et al. (1989)
	"	C+P	Levenspiel et al. (1970) only monotonic case; present paper: non-monotonic case
	Bingham	F	Zakharov (2006)
	Ostwald-de Waele	C	Foraboschi and Vaccari (1965)
	"	F	Zakharov (2006)
	Prandtl-Eyring	F	Sawinsky and Simandi (1983)
	Generalized root law	G	Present paper
Circular pipe	Newtonian	P	Bosworth (1948), Danckwerts (1953)
	"	P+E	Hsu and Wei (2005)
	Bingham	P	Wein and Ulbrecht (1972)
	Casson	P	Sawinsky and Balint (1984)
	Ostwald-de Waele	P	Foraboschi and Vaccari (1965), Novosad and Ulbrecht (1966)
	Herschel-Bulkley	P	Wein and Ulbrecht (1972)
	Prandtl-Eyring	P	Wein and Ulbrecht (1972)
	Rabinowitsch	P	Wein and Ulbrecht (1972)
	Generalized root law	G	Bosworth (1949)
	Generalized exponential and sinusoidal law	G	Pegoraro et al. (2012)
Concentric annulus	Newtonian	P	Nigam and Vasudeva (1976) in implicit form; present paper: explicit form
	Ostwald-de Waele	P	Lin (1980) approximate; Pechoč (1983) numerical

Table 2: Function f and related quantities for generalized monotonic velocity profiles.

	Power law $(q > 0)$	Root law $(m \geq 1)$	Couette-Poiseuille flow $(0 < s \leq 1)$
$f(x)$	$\dfrac{1-x^q}{\theta_\mathrm{F}}$	$\dfrac{(1-x)^{1/m}}{\theta_\mathrm{F}}$	$\dfrac{1}{\theta_\mathrm{W}}(1-x)(1+sx)$
$f^{-1}(x)$	$\left(1-\theta_\mathrm{F}x\right)^{1/q}$	$1-(\theta_\mathrm{F}x)^m$	$\dfrac{(s-1)+\sqrt{(s-1)^2+4s(1-\theta_\mathrm{W}x)}}{2s}$
$f'(x)$	$-\dfrac{q}{\theta_\mathrm{F}}x^{q-1}$	$-\dfrac{(1-x)^{(1-m)/m}}{m\theta_\mathrm{F}}$	$-\dfrac{1-s+2sx}{\theta_\mathrm{W}}$
$G(x)=\int f\mathrm{d}x$	$\dfrac{x}{\theta_\mathrm{F}}\left(1-\dfrac{x^q}{q+1}\right)$	$-\dfrac{m(1-x)^{(m+1)/m}}{(m+1)\theta_\mathrm{F}}$	$\dfrac{x}{\theta_\mathrm{W}}\left(1-\dfrac{1-s}{2}x-\dfrac{s}{3}x^2\right)$
$H(x)=\int G\mathrm{d}x$	$\dfrac{x^2}{2\theta_\mathrm{F}}\left(1-\dfrac{2x^q}{(q+1)(q+2)}\right)$	$\dfrac{m^2(1-x)^{(2m+1)/m}}{(m+1)(2m+1)\theta_\mathrm{F}}$	$\dfrac{x^2}{2\theta_\mathrm{W}}\left(1-\dfrac{1-s}{3}x-\dfrac{s}{6}x^2\right)$
θ_F plane channel	$\dfrac{q}{q+1}$	$\dfrac{m}{m+1}$	$\theta_\mathrm{F}=\theta_\mathrm{W}=\dfrac{3+s}{6}$
θ_F circular pipe	$\dfrac{q}{q+2}$	$\dfrac{2m^2}{(m+1)(2m+1)}$	